SimBuild
2024

Eleventh National Conference of IBPSA-USA
Denver, Colorado
May 21 – 23, 2024

# Assessing the Impact of Variable Air Volume Box Damper Stuck Faults Using a Building Automation System and Building Energy Simulation Model

Sungkyun Jung[1], Yeobeom Yoon[1], Piljae Im[1]
[1]Oak Ridge National Laboratory, Oak Ridge, TN

## Abstract

The study examines the impact of variable air volume (VAV) damper stuck faults on the system operation, building indoor conditions, and reheating energy consumption. This study includes both experimental and simulation studies for five test scenarios, including a fault-free scenario. We implemented VAV damper stuck fault through the building automation system (BAS). Results show that a damper stuck in a high opening position (60% damper opening) results in supplying an excessive amount of cold air from the rooftop unit (RTU) to the conditioned zone, increasing reheating energy consumption. The results of this research can serve as a foundational resource for developing fault detection algorithms.

## Introduction

Faults with heating, ventilation, and air-conditioning (HVAC) systems, such as deviations from their intended operating conditions, can lead to higher energy usage and operational expenses for a building. Additionally, these faults might hinder the HVAC services a building requires, impact other linked energy systems negatively, and potentially raise costs for equipment maintenance or replacement (Ebrahimifakhar et al., 2021). Faults in HVAC systems contribute to a significant waste of energy, amounting to as much as 30% of energy consumption in commercial buildings. These faults have a negatively effect on system efficiency and the lifespan of HVAC equipment. (Fernandez et al, 2012; Granderson et al., 2017; Zhang et al., 2021).

*This manuscript has been authored by UT-Battelle, LLC, under contract DE-AC05-00OR22725 with the US Department of Energy (DOE). The US government retains and the publisher, by accepting the article for publication, acknowledges that the US government retains a nonexclusive, paid-up, irrevocable, worldwide license to publish or reproduce the published form of this manuscript, or allow others to do so, for US government purposes. DOE will provide public access to these results of federally sponsored research in accordance with the DOE Public Access Plan (http://energy.gov/downloads/doe-public-access-plan).*

Research efforts are underway to develop methods for fault detecting and diagnostic (FDD) in HVAC systems due to their significant impact on energy consumption (Najafi, 2010; Frank et al., 2019). However, the development and evaluation of these FDD methods require comprehensive historical operation data from both fault and fault-free states. Gathering high-resolution and high-quality data from actual buildings with faults presents a notably difficult task. Moreover, collecting both fault and fault-free data from the same building under the same building operating conditions is also challenging. The shortage of data impedes the progress and assessment of FDD algorithms and techniques. (Chen et al., 2022). Consequently, only a handful of previous studies have utilized historical operation data from buildings with faults to develop and evaluate FDD methods (Frank et al., 2019; Granderson et al., 2018; Shoukas et al., 2020).

In the current commercial building sector, variable-air volume (VAV) terminal unit, typically called a VAV box, are preferred because of their ability to adjust to the fluctuating thermal load and ventilation requirements of a building. It makes VAV systems a widely chosen and popular option (Okochi and Yao, 2016; Pang et al., 2017). VAV box comprises a motorized damper, temperature and airflow rate sensors, and reheating coils. The VAV box controller employs two control loops: one for maintaining indoor air temperature and another for controlling airflow rate (Wang et al., 2021). The significance of the VAV box is evident as it directly influences building indoor conditions.

VAV box often encounter issues related to damper operation and airflow rate sensor faults (Ebrahimifakhar, 2021; Wang et al., 2021). Qin and Wang delved into the functionality of VAV boxes and revealed instances where measured airflow and indoor air temperature failed to meet the set objectives. Following a comprehensive evaluation, 261 out of 1,251 VAV boxes

(20.9%) were identified as potentially problematic (Qin and Wang, 2005).

Nevertheless, there was a scarcity of publicly accessible VAV box data and its analysis.

In this research, we implemented a VAV box damper opening stuck fault into a commercial building test facility using a Building Automation System (BAS) to generate fault data. We then analyzed this fault data to assess the impact of the VAV box damper opening stuck fault on building indoor conditions and HVAC system operation in an actual commercial building test facility. Additionally, we developed and calibrated building energy simulation models using both fault-free data and fault data. Through these simulations, we were able to evaluate the potential annual energy consumption impact caused by the VAV box damper opening stuck fault.

## Methodology

Experimental and simulation studies were conducted to understand the impact of the VAV box damper stuck on building indoor conditions and HVAC system operation. In this section, we describe the test building and the simulation model development.

For this study, we undertook fault-free (baseline) and fault scenario testing, with a specific focus on VAV damper stuck with various damper opening positions. To accomplish this, we conducted tests at a test facility, allocating one day to each scenario involving damper stucking at a specific opening position, and collected the test data. Following the testing phase, we developed the fault (VAV damper stuck) models using building energy simulation program based on the collected data. Finally, using these fault models, we conducted a comprehensive analysis of the impact of VAV damper faults on both indoor air temperature and heating energy consumption within a specific room.

### Test facility

The Flexible Research Platform (FRP) at Oak Ridge National Laboratory (ORNL) has been selected as a test facility for this study. ORNL's FRP is a research facility with multiple zones, specifically designed to emulate light commercial buildings typically found in the United States. Within ORNL's FRP, over 500 sensors have been deployed. This facility is well-known for its role as a commercial building test facility, where various field tests have been carried out. Additionally, some of the field datasets collected at ORNL's FRP are available to the public (Granderson et al., 2020; Yoon et al., 2022; Granderson et al., 2023).

Table 1 shows construction information of the FRP building, including the exterior walls, roofs, windows, doors, floors, as well as interior walls.

*Table 1 Construction characteristics*

| Construction | Thermal characteristics |
|---|---|
| **Wall structure** | Concrete masonry units with face brick |
| **Wall insulation** | Fiberglass $R_{SI}$-1.9 ($m^2$-K/W) ($R_{US}$-11 (Btu/(h-F-$ft^2$))) (Moderate level of efficiency) |
| **Floor** | Slab-on-grade |
| **Roof structure** | Metal deck with polyisocyanurate and ethylene propylene diene monomer |
| **Roof insulation** | Polyisocyanurate $R_{SI}$-3.17 ($R_{US}$-18) (Moderate level of efficiency) |
| **Windows** | Double clear glazing with aluminum frame |
| **Window-to-wall ratio** | 29% |

Figure 1 illustrates the HVAC system diagram. Within the FRP building, a Rooftop Unit (RTU) system has been installed, which comprises a variable-speed evaporator fan and a direct expansion (DX) cooling coil. The RTU system is connected to VAV terminal units, and each VAV unit includes reheat coils and dampers. Since the FRP building is divided into 10 conditioned zones, 10 VAV terminal units were installed.

For this research, we chose a room that faces the south and east sides as the designated space for conducting VAV damper stuck tests.

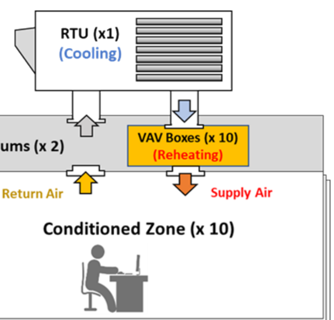


*Figure 1 Diagram of the HVAC system operation*

### VAV damper stuck tests

In the process of collecting and analyzing VAV damper being stuck data, tests were conducted in both VAV damper stuck and non-stuck (fault-free) conditions.

Initially, a scenario with fault-free conditions was established for comparison with a faulty situation. To create a fault-free scenario, we replicated the standard operation of a typical commercial building where dampers are unobstructed. The heating setpoint is 21°C (69.8°F) and the cooling setpoint is 24°C (75.2°F) during occupied hours, which are from 7 a.m. to 10 p.m. During unoccupied hours, which are from 10 p.m. to 7 a.m., these settings were adjusted to 15.6°C (60°F) for heating and 29.4°C (85°F) for cooling. Fault-free testing involved utilizing a RTU to maintain a consistent supply air temperature of 12.8°C (55°F).

To investigate the impact of varying degrees of VAV damper being stuck, scenarios were established with damper positions set at intervals of 20%, ranging from 0% to 60%. These configurations were implemented using the BAS, and daily tests were conducted to implement and test the opening levels. These tests maintained consistent building operations with the fault-free tests, differing solely in the presence of the stuck conditions.

Fault tests were carried out in August 2023, with specific details outlined in Figure 2 and Table 2.

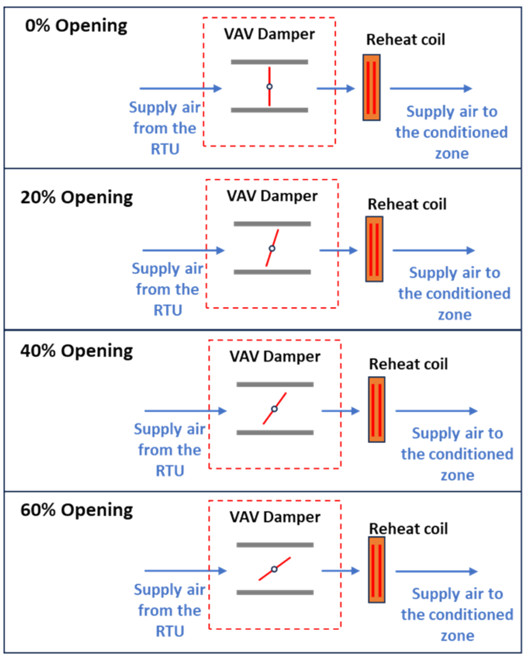


*Figure 2 VAV damper stuck scenarios*

*Table 2 Test scenarios*

| Test date | Test scenario |
|---|---|
| 8/3/2023 | Fault-free test |
| 8/4/2023 | VAV damper stuck at 0% open |
| 8/5/2023 | VAV damper stuck at 20% open |
| 8/6/2023 | VAV damper stuck at 40% open |
| 8/7/2023 | VAV damper stuck at 60% open |

Considering the assumption that simultaneous VAV damper stuck occurrences would be infrequent, the test was conducted in a single room: one located in the south, chosen from a total of 10 conditioned rooms in the facility. Furthermore, the decision to focus on only one room stemmed from our intention to avoid any exaggeration in the results pertaining to VAV damper stuck. Throughout the fault tests, the other rooms sustained fault-free conditions.

At first, we examined the typical occupancy density and operational timetable. We accounted for sensible heat generated by occupants and various office equipment, such as computers, monitors, and copiers, by using portable heaters and timers. The latent heat emitted by occupants was introduced utilizing a humidifier along with timers. Furthermore, a specialized control system was employed to regulate the interior lighting fixtures, allowing them to be activated and deactivated according to a standard office operational schedule.

**Fault model development**

The inputs for the building energy simulation model were derived from as-built drawings, nominal performance data, and performance tests for elements such as the roof, exterior walls, and windows. Using these inputs, an EnergyPlus model of the test building was developed and subsequently calibrated using both fault-free and fault test data.

The VAV terminal unit consists of a VAV damper and a reheating coil. It regulates the opening of the VAV damper and the on/off operation of the reheating coil based on the heating and cooling thermostat setpoint temperatures. The VAV terminal unit reduces the damper opening to minimize airflow rate and activates the reheating coil for heating purposes. In contrast, during cooling, the reheating coil remains off, while the damper opening is increased to raise the supply airflow rate, thereby adjusting the degree of cooling. When the indoor air temperature is between the cooling and heating setpoint temperatures, the reheating coil remains off, and only the damper is opened minimally.

To verify the proper functioning of the VAV damper, an analysis was conducted using measured data to ensure that the cooling, heating, and deadband modes of the VAV terminal unit were operating correctly in accordance with thermostat temperature setpoints and indoor air temperature. To validate fault-free and fault building energy simulation models of the VAV damper, the indoor air temperature, supply airflow rate, and heating energy consumption from both measured and simulated data were compared.

For the validation of the simulation model, we used weather files generated from data collected by sensors at a dedicated weather station installed on the roof of the test building. These sensors measured various parameters including direct normal irradiation, diffuse horizontal irradiance, global horizontal irradiance, outdoor air temperature and humidity, wind speed, wind direction, precipitation, and atmospheric pressure.

This study employed the normalized mean bias error (NMBE) and the coefficient of variation of the root mean square error (cv(RMSE)) as metrics for quantifying the disparities between measurements and simulations in the simulation model validation process. Both metrics express the percentage deviation, with lower values signifying more accurate simulation results. The NMBE, considering its sign, can assist in identifying overfitting or underfitting issues. The cv(RMSE) provides insight into the consistency or stability of the model's predictive performance across different subsets of data or across multiple runs. In accordance with American Society of Heating, Refrigerating and Air Conditioning Engineers (ASHRAE) Guideline 14-2014, an acceptable threshold for cv(RMSE) is below 30%, and for NMBE, falling within the range of ±10% (ASHRAE 2014).

$$NMBE = \frac{\frac{1}{N}\sum_{i}^{N}(y_i - \hat{y}_i)}{\bar{y}} \times 100 \tag{1}$$

$$\text{cv(RMSE)} = \frac{\sqrt{\frac{1}{N}\sum_{i}^{N}(y_i - \hat{y}_i)^2}}{\bar{y}} \times 100 \tag{2}$$

In the given expressions, $y_i$ representes the measured data value, $\hat{y}_i$ represents the predicted (simulated) value, $\bar{y}$ represents the average of the $y_i$, N represents the total number of data points.

### Fault status impact analysis

To analyze the impact of the VAV damper stuck fault, developed fault simulation models were utilized. The simulations, initially conducted for one day for calibration, were extended to annual simulations to assess the impact of the VAV damper stuck fault on building indoor conditions and HVAC system operations. For this analysis, a Typical Meteorological Year 3 (TMY3) weather file for Knoxville, TN was used.

It is important to highlight that the fault-free and fault simulation models were created using data collected in the month of August. Therefore, the analysis in this study only focuses on the summer season (June, July, August, and September), aligning with the measured data. As mentioned earlier, the VAV terminal unit controls both the supply air temperature and supply airflow rate to maintain the indoor air temperature setpoints. Additionally, the energy consumption of the reheating coil in the VAV terminal unit is determined by both the supply air temperature and the supply airflow rate. Therefore, the purpose of this analysis is to understand how the degree of damper stuck affects reheating energy consumption and indoor air temperature, considering that VAV terminal units control the supply air temperature and the airflow rate.

## Results and Discussions

### Test data analysis

The fault-free and fault tests, as discussed in earlier sections, were conducted over a span of five days from August 3rd to the 7th. August 3rd was dedicated to a fault-free test. Subsequent days involved testing the damper in different fault scenarios: fully closed position (0% open) on the 4th, stuck at 20% open on the 5th, at 40% open on the 6th, and in the open position at 60% on the 7th.

Throughout this testing period, the outdoor air temperature ranged from 19.1°C (66.4°F) to 31.7°C (89.1°F) (Figure 3). The data were collected at a 1-minute resolution during this testing period for analysis purposes.

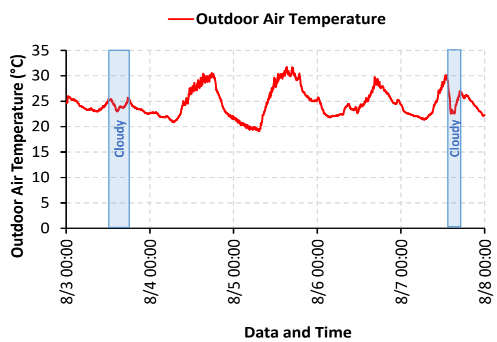


*Figure 3 Outdoor air temperature during the test period*

In the VAV damper stuck test, a substantial rise in indoor air temperature occurred on August 4th and 5th when the damper was either not fully closed (0%) or only partially opened to 20% (Figure 4). This occurrence becomes particularly noticeable when the VAV damper is fully closed, preventing the delivery of cold air from the RTU to the zone for cooling. In other words, when the damper is stuck at 0% opening, the VAV terminal unit functions as if its cooling capability has been turned off. Despite this, the temperature did not increase significantly compared to the outdoor air temperature. This suggests that the temperature of the test room may have been influenced by the air temperature in adjacent rooms and the plenum. In other test cases, the temperature remained within the cooling and heating setpoint temperatures.

During the fault-free test on August 3rd, the damper operated at approximately 40% opening. This corresponds to the condition where a 40% opening is sufficient to meet the VAV minimum airflow requirement. On this day, most of the time, the system met the cooling and heating setpoint temperatures with the minimum airflow, and there was no need for additional cooling. Therefore, there was no reason for the damper to open more extensively. Additionally, it can be observed that the airflow in the damper stuck test at 40% is similar to that in the fault-free test.

Lastly, upon closer examination of the indoor air temperature on August 8th, when the damper was 60% opened, it was observed that the indoor air temperature was relatively lower compared to when the damper was less open. This suggests that, even on the day when additional cooling may not be necessary, the damper allowed more cold air from the RTU to enter than the minimum airflow required.

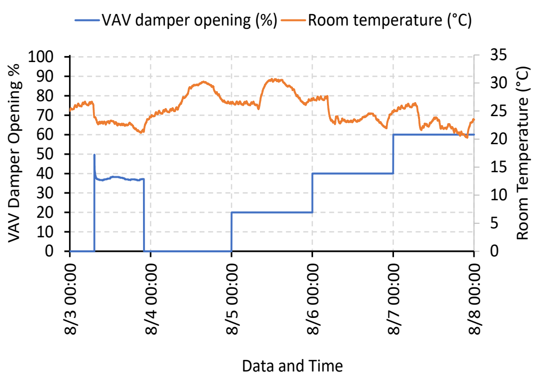


*Figure 4 Indoor air temperature with VAV damper opening*

As illustrated in Figure 5, it is clear that the reheating energy consumption was minimized. On August 4th, when the damper was at 0%, as previously stated, neither cooling nor reheating was active, resulting in a reheating energy consumption reading of 0. Throughout August 5th to the 7th, the reheating coil stayed dormant, signaling the absence of a reheating demand during the summer test period. Nonetheless, during the fault-free test on August 3rd, a slight amount of reheating energy was utilized right before entering the unoccupied hour.

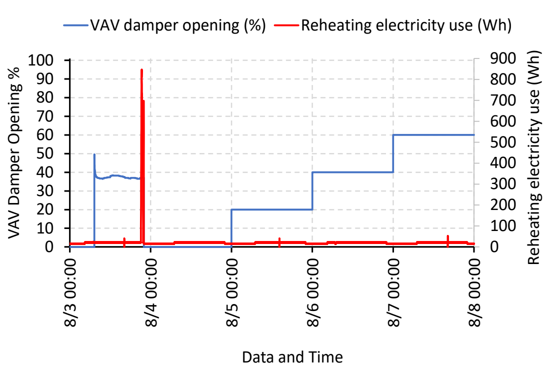


*Figure 5 Reheating energy consumption with VAV damper opening*

**Fault status simulation model**

Given that the VAV terminal unit plays a pivotal role in determining reheating and cooling, the precision of the simulation model becomes paramount. Consequently, within this section, a thorough comparison between the simulation results and actual measurements was undertaken for each test case to gauge their alignment.

The simulation model outputs under fault-free conditions, encompassing indoor air temperature, supply airflow rate, and reheating energy consumption, were assessed against the measurements presented in Figures 6, and 7.

In the fault-free test scenario, the simulation results were compared to the measured data, especially, indoor air temperatures, supply airflow rate, and reheating energy consumption. The simulation results closely match the measured data. The cv(RMSE) and NMBE for indoor air temperatures were found to be 0.6% and -0.1%, for supply airflow rate were 5% and -2%, and for reheating energy consumption were 2.7% and -2.5%.

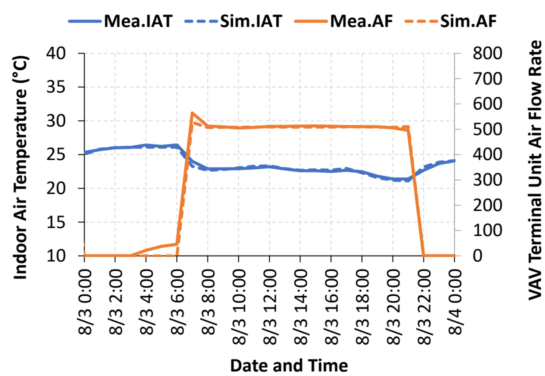


*Figure 6 Measured and simulated indoor air temperatures and supply airflow rates during the fault-free test*

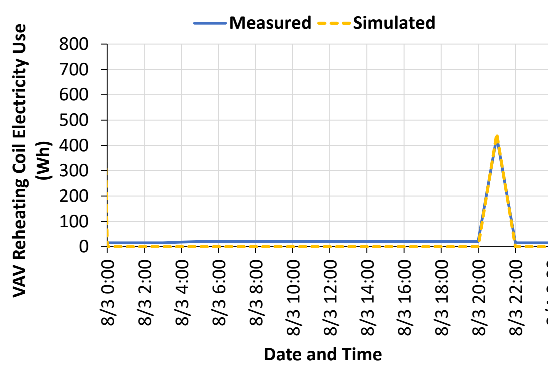


*Figure 7 Measured and simulated reheating energy usage during the fault-free test*

The simulation results under the 0% open damper stuck test, encompassing indoor air temperature, and supply airflow rate, were assessed against the measured data presented in Figure 8. Due to the absence of reheating energy consumption, the graph depicting reheating energy has been omitted. The simulation results closely align with the measurements. In the 0% open damper stuck scenario, the simulated values for indoor air temperatures and supply airflow rate, were compared to the measured data. The cv(RMSE) and NMBE for indoor air temperatures were found to be 2.1% and 0.1%, and for supply airflow rate were 12% and -0.8%.

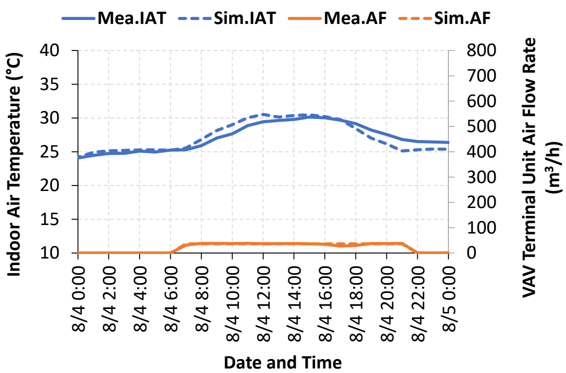


*Figure 8 Measured and simulated indoor air temperatures and supply airflow rates during the 0% open damper stuck test*

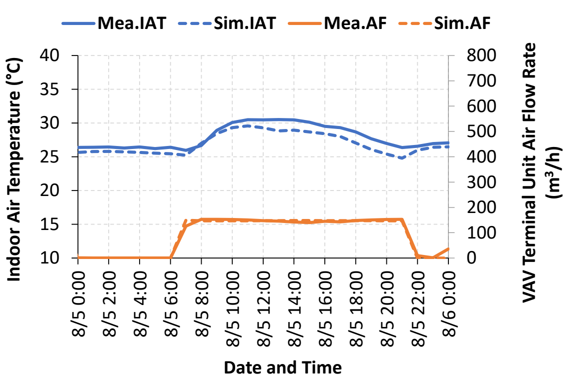


*Figure 9 Measured and simulated indoor air temperatures and supply airflow rates during the 20% open damper stuck test*

The simulation results for the 20% open damper stuck test, covering indoor air temperature and supply airflow rate, were compared with the measured data depicted in Figure 9. Since there was no reheating energy consumption, the graph illustrating reheating energy has been excluded. The simulation results closely align with the measurements. In the scenario with a 20% open damper stuck, the simulated results were compared with measured data especially, indoor air temperatures and supply airflow rate. The cv(RMSE) and NMBE for indoor air temperatures were determined to be 2.5% and -2.3%, and for supply airflow rate were 10.6% and -1.7%, respectively.

The simulation results for the 40% open damper stuck test, encompassing indoor air temperature and supply airflow rate, were compared with the data presented in Figure 10. Owing to the absence of reheating energy consumption, the chart representing reheating energy has been excluded. The simulation results closely correspond with the measurements, as evidenced by the results of cv(RMSE) and NMBE. In the case of the 40% open damper stuck scenario, the simulated values for indoor air temperatures and supply airflow rate were compared with the measured data. The cv(RMSE) and NMBE for indoor air temperatures were found to be 1.5% and -0.6%, and for supply airflow rate were 13.4% and -2.1%, respectively.

Analyzing Figure 10 unveils a unique trend in contrast to test data from other fault scenarios. In this case, the HVAC system turned on before the scheduled occupancy hour, resulting in cold airflow into the room. This occurrence is attributed to the indoor air temperature in other rooms failing to reach the thermostat setpoint, triggering the HVAC system to activate prematurely.

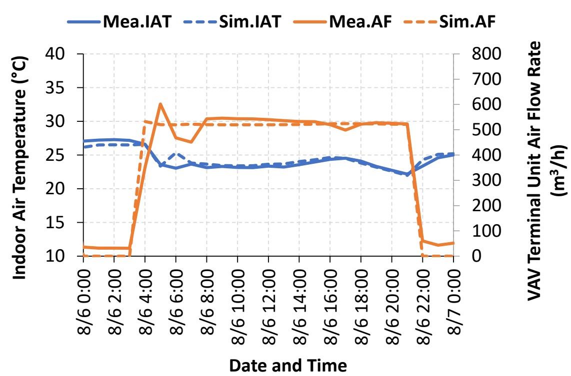


*Figure 10 Measured and simulated indoor air temperatures and supply airflow rates during the 40% open damper stuck test*

The simulation results for the 60% open damper stuck test, covering indoor air temperature and supply airflow rate, were compared with the data presented in Figure 11. Since there was no reheating energy consumption, the graph illustrating reheating energy has been excluded. The simulation results closely align with the measurements. In the scenario with a 60% open damper stuck, the simulated values for indoor air temperatures and supply airflow rate were contrasted with the measured data. The cv(RMSE) and NMBE for indoor air temperatures were determined to be 1.6% and 0.7%, and for supply airflow rate were 12.1% and -3.2%, respectively.

As demonstrated in this section, both the fault-free and fault models were developed based on measured data, and all the models have been well calibrated.

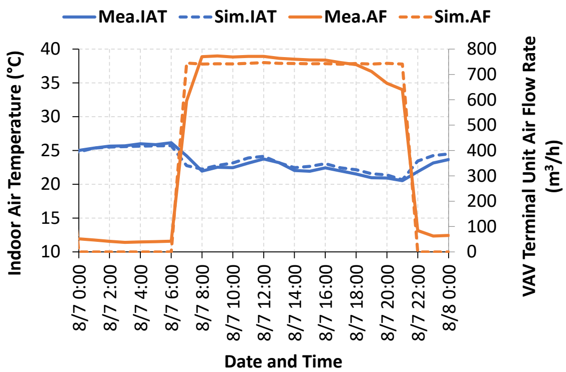


*Figure 11 Measured and simulated indoor air temperatures and supply airflow rates during the 60% open damper stuck test*

### Fault status impact analysis

Using the model created in the prior section, annual analysis was conducted to examine the consequences of damper stuck in VAV terminal units. In this study, only the summer season was taken into account, as the measured data used for developing the simulation models pertained to summer conditions.

Figures 12 and 13 depict the results of reheating energy consumption and indoor air temperature for the fault-free model and the damper stuck at 0% open model.

The fault-free (baseline) model used 24.7 kWh for reheating in June, 7.1 kWh in July, 8.6 kWh in August, and 71.8 kWh in September. The highest reheating energy consumption is observed in September, which is attributed to the lowest average outdoor air temperature and relatively lower solar radiation compared to other months.

In the damper stuck at 0% open condition, there was almost no airflow for reheating, resulting in a reheating energy consumption of 0. In this scenario, the indoor air temperature was higher than the fault-free condition because the closed damper prevented the inflow of cold air from the RTU. As a result, the indoor air temperature was higher than in the fault-free condition, depending on the outdoor air temperature and solar radiation.

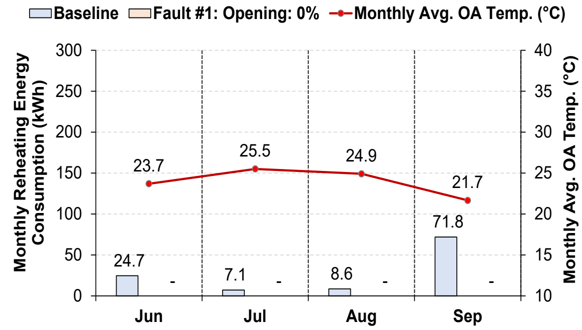


*Figure 12 Monthly averaged outdoor air temperature and reheating energy consumption (Baseline: fault-free condition vs. Damper stuck at 0% open)*

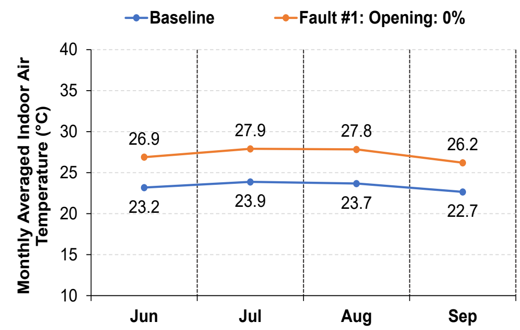


*Figure 13 Monthly averaged indoor air temperature (Baseline: fault-free condition vs. Damper stuck at 0% open)*

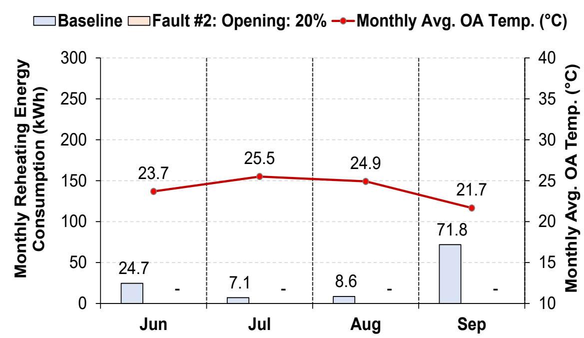


*Figure 14 Monthly averaged outdoor air temperature and reheating energy consumption (Baseline: fault-free condition vs. Damper stuck at 20% open)*

Figures 14 and 15 illustrate the outcomes of reheating energy consumption and indoor air temperature for the damper stuck at 20% open model. In the damper stuck at 20% open condition, insufficient airflow prevented the indoor air temperature from dropping below the heating setpoint temperatures, resulting in a reheating energy consumption of 0. In this scenario, the indoor air temperature surpassed that of the fault-free condition due to the 20% damper open restricting the adequate inflow of cold air from the RTU. Consequently, the indoor air temperature was higher than in the fault-free condition, contingent on the outdoor air temperature and solar radiation.

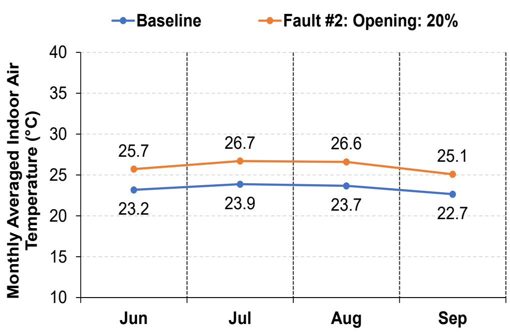


*Figure 15 Monthly averaged indoor air temperature (Baseline: fault-free condition vs. Damper stuck at 20% open)*

Figures 16 and 17 present the results of reheating energy consumption and indoor air temperature for the damper stuck at 40% open model. In the damper stuck at 40% open condition, this opening is nearly identical to the fault-free condition, leading to a reheating energy consumption similar to that of the fault-free model. Consequently, the indoor air temperatures in this scenario closely resemble those of the fault-free model. In 40% damper stuck scenario, the reheating energy consumption has increased by approximately 7% to 14% each month compared to the baseline. Overall, the reheating energy consumption in this faulty scenario is about 9% higher than that in the baseline.

Figures 18 and 19 illustrate the results of reheating energy consumption and indoor air temperature for the stuck damper in the 60% open model. With the damper 60% open, excessive air flow led to a drop in indoor air temperature, resulting in increased reheating energy consumption. In this scenario, the indoor air temperature was slightly lower than the fault-free model since it still met the heating setpoint temperature. However, if the heating coil capacity is insufficient to handle the high air flow rate, the indoor air temperature could potentially fall below the heating setpoint temperature. In 60% damper stuck scenario, the reheating energy consumption has increased by approximately 207% to 890% each month compared to the baseline. Overall, the reheating energy consumption in this faulty scenario is about 338% higher than that in the baseline.

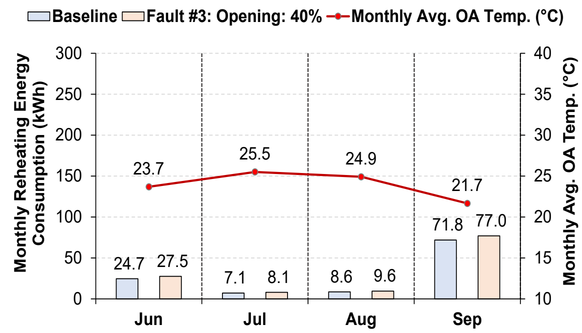


*Figure 16 Monthly averaged outdoor air temperature and reheating energy consumption (Baseline: fault-free condition vs. Damper stuck at 40% open)*

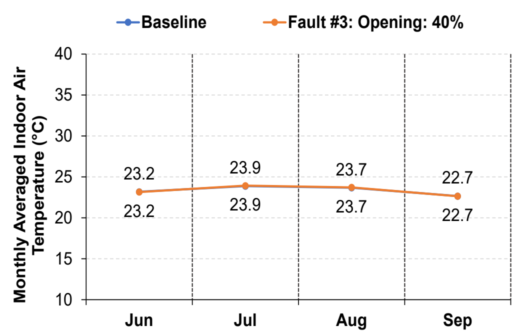


*Figure 17 Monthly averaged indoor air temperature (Baseline: fault-free condition vs. Damper stuck at 40% open)*

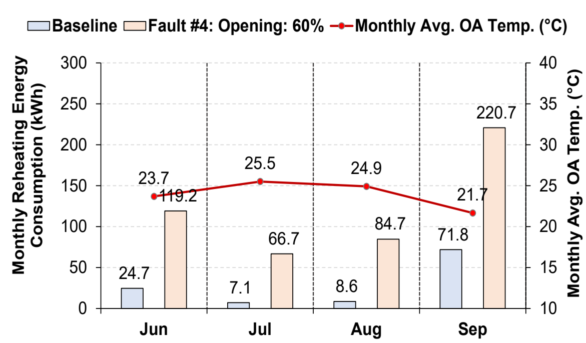


*Figure 18 Monthly averaged outdoor air temperature and reheating energy consumption (Baseline: fault-free condition vs. Damper stuck at 60% open*

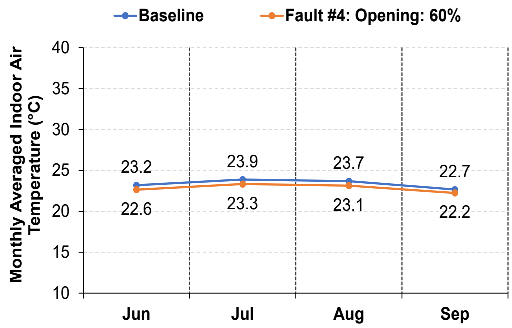


*Figure 19 Monthly averaged indoor air temperature (Baseline: fault-free condition vs. Damper stuck at 60% open)*

## Conclusion

This study outlines a comprehensive procedure for generating datasets depicting HVAC fault status, specifically focusing on VAV damper stuck, using the BAS system. This approach addresses data scarcity challenges in FDD. Applying HVAC faults directly for implementation instead of using the BAS system to simulate faults is costly and poses potential risks to the building or HVAC system. In contrast, utilizing the BAS system to generate fault data is a cost-, and time-effective, and safe alternative.

We additionally demonstrate a simulation technique for generating HVAC fault data based on one-day data. While this method can produce more data than the measured data, caution is necessary. Using one day of data for each case may not suffice to generalize fault behaviors. Specifically, this study relied solely on cooling season data for generating simulated data, which does not encompass the heating season and shoulder seasons. Conducting seasonal tests is essential to generate data that spans all seasons. Furthermore, an important consideration in this study pertains to the selection of a single space for testing and the development of the simulation model. This room, sharing indoor air temperature, leakage, and plenum space variables with neighboring rooms, requires careful attention. When designing building energy simulations, meticulous consideration should be given to the temperatures of adjacent rooms and the plenum.

Finally, in this study, we examined monthly simulation outcomes by considering the damper open percentage in a stuck position to comprehend its effects on the building's energy consumption and indoor air temperature. As a result, when the damper was stuck at 0%, neither reheating nor cooling operations were functioning. Particularly in the summer season with high outdoor air temperatures, the lack of cooling led to an increase in indoor air temperature. When the damper was stuck at 20%, there was a modest airflow of approximately 150m$^3$/h, resulting in a slightly lower indoor air temperature compared to when the damper was stuck at 0%. However, as the indoor air temperature still did not reach the heating setpoint, and there was no reheating energy consumption. Additionally, during daytime hours with high outdoor air temperatures and significant solar radiation, the insufficient airflow led to an increase in indoor air temperature. When the damper was stuck at 40%, the airflow rate was similar to the fault-free condition (approximately 520 m$^3$/h). Consequently, the indoor air temperature pattern and reheating energy consumption were also similar. Finally, when the damper was stuck at 60%, the airflow rate exceeded the required amount. If there had been no reheating operation, the indoor air temperature would have likely dropped to the lowest point. The 60% damper opening excessively supplied cold air from the RTU, leading to excessive reheating energy consumption.

In the near future, we plan to conduct a damper stuck fault test during the heating season to understand the impact of damper malfunctions on indoor conditions, HVAC system operation, and energy consumption. Additionally, we will conduct tests for other types of faults typically observed in commercial buildings, generating fault-free and faulty datasets.

## Acknowledgment

This material is based upon work supported by the US Department of Energy's (DOE's) Office of Science and Building Technologies Office (BTO). This research used resources of Oak Ridge National Laboratory's Building Technologies Research and Integration Center, which is a DOE Office of Science User Facility. This work was funded by fieldwork proposal CEBT105 under BTO activities BT0302000 and BT0305000. This manuscript has been authored by UT-Battelle LLC under contract DEAC05-00OR22725 with DOE. The US government retains and the publisher, by accepting the article for publication, acknowledges that the US government retains a nonexclusive, paid-up, irrevocable, worldwide license to publish or reproduce the published form of this manuscript, or allow others to do so, for US government purposes.

## References

ASHRAE. (2014). ASHRAE Guideline 14-2014, Section 5.3.3.3.10, American Society of Heating, Refrigerating and Air-Conditioning Engineers.

Chen, J., Zhang, L., Li, Y., Shi, Y., Gao, X., & Hu, Y. (2022). A review of computing-based automated fault detection and diagnosis of heating, ventilation and air conditioning systems. Renewable and Sustainable Energy Review, 161.

Ebrahimifakhar, A. (2021), Investigation of the Prevalence of Faults in the Heating, Ventilation, and Air-Conditioning Systems of Commercial Buildings, PhD dissertation, University of Nebraska-Lincoln.

Ebrahimifakhar, A., Yuill, D., Smith, A., Granderson, J., & Crowe, E. (2021). Analysis of automated fault detection and diagnostics records as an indicator of HVAC fault prevalence: Methodology and preliminary results. International High Performance Buildings Conference at Purdue, West Lafayette, IN.

Fernandez, N., Katipamula, S., Wang, W., Huang, Y., & Liu, G. (2012). Energy savings modeling of standard commercial building re-tuning measures: large office buildings (No. PNNL-21569). Pacific Northwest National Laboratory, Richland, WA.

Frank, S., Lin, G., Jin, X., Singla, R., Farthing, A., & Granderson, J. (2019). A performance evaluation framework for building fault detection and diagnosis algorithms. Energy and Buildings, 192.

Granderson, J., Lin, G., Chen, Y., Casillas, A., Chen, Z., Im, P., Huang, S., & Ling, J. (2023). A labeled dataset for building HVAC systems operating in faulted and fault-free states, Scientific Data, 10, 1-13.

Granderson, J., Lin, G., Harding, A., Im, P., & Chen, Y. (2020). Building fault detection data to aid diagnostic algorithm creation and performance testing, Scientific Data, 7, 1-14.

Granderson, J., Lin, G., Singla, R., Mayhorn, E., Ehrlich, P., & Vrabie, D. (2018). Commercial fault detection and diagnostics tools: What they offer, how they differ, and what's still needed. 2018 ACEEE summer study on energy efficiency in buildings.

Granderson, J., Singla, R., Mayhorn, E., Ehrlich, P., Vrabie, D., & Frank, S. (2017). Characterization and survey of automated fault detection and diagnostic tools. Lawrence Berkeley National Laboratory. Report No. LBNL-2001075.

Najafi, M. (2010) Fault detection and diagnosis in building HVAC systems. PhD dissertation, University of California, Berkeley.

Okochi, G. S. & Yao, Y. (2016) A review of recent developments and technological advancements of variable-air-volume (vav) air-conditioning systems, Renewable and Sustainable Energy Reviews, 59, 784-817.

Pang, X., Piette, M. A., & Zhou, N. (2017). Characterizing variations in variable air volume system controls, Energy and Buildings, 135, 166–175.

Qin, J. & Wang, S. (2005) A fault detection and diagnosis strategy of VAV air-conditioning systems for improved energy and control performances, Energy and Buildings, 37, 1035–1048.

Shoukas, G., Bianchi, M., & Deru, M. (2020). Analysis of fault data collected from automated fault detection and diagnostic products for packaged rooftop units. National Renewable Energy Laboratory. Report No. NREL/TP-5500-77077.

Wang, H., Feng, D., & Liu, K. (2021). Fault detection and diagnosis for multiple faults of VAV terminals using self-adaptive model and layered random forest, Building and Environment, 193, 107667.

Yoon, Y., Jung, S., Im, P., & Gehl, A. (2022). Datasets of a Multizone Office Building under Different HVAC System Operation Scenarios. Scientific Data, 9, 1-11.

Zhang, L., Leach, M., Bae, Y., Cui, B., Bhattacharya, S., Lee, S., Im, P., Adetola, V., Vrabie, D., & Kuruganti, T. (2021). Sensor impact evaluation and verification or fault detection and diagnostics in building energy systems: A review. Advances in Applied Energy, 3.